The effect of hybridization on local magnetic interactions at highly diluted Ce ions in tetragonal intermetallic compounds $RERh_2Si_2$ (RE=Ce, Pr, Nd, Gd, Tb, Dy)

2012 J. Phys.: Condens. Matter 24 416002

(http://iopscience.iop.org/0953-8984/24/41/416002)

J. Phys.: Condens. Matter **24** (2012) 416002 (11pp) doi:10.1088/0953-8984/24/41/416002

The effect of hybridization on local magnetic interactions at highly diluted Ce ions in tetragonal intermetallic compounds $RERh_2Si_2$ (RE = Ce, Pr, Nd, Gd, Tb, Dy)

G A Cabrera-Pasca, A W Carbonari, B Bosch-Santos, J Mestnik-Filho and R N Saxena

Instituto de Pesquisas Energéticas e Nucleares, IPEN-CNEN/SP, Avenue Professor Lineu Prestes, 2242, 05508-000 São Paulo, Brazil

E-mail: carbonar@ipen.br

Received 14 June 2012, in final form 31 August 2012
Published 24 September 2012
Online at stacks.iop.org/JPhysCM/24/416002

Abstract

The contribution of the 4f electron to the local magnetic field at highly diluted Ce atoms in $RERh_2Si_2$ (RE = Ce, Pr, Nd, Gd, Tb, Dy) has been investigated as a function of temperature through the measurement of the magnetic hyperfine field in ^{140}Ce nuclei by time differential perturbed gamma–gamma angular correlation spectroscopy. Samples of the studied compounds were characterized by x-ray diffraction and zero-field resistance to determine the crystal structure and transport properties. DC magnetic susceptibility was measured for $NdRh_2Si_2$. It was observed that the variation of the magnetic hyperfine field with temperature follows the expected behaviour for the host magnetization, with the exception of $GdRh_2Si_2$, which showed a strong deviation from such a behaviour. It is shown that the hybridization of the d band of the host with the f band of the Ce impurity, which is stronger in $GdRh_2Si_2$ than in other compounds, is responsible for the observed deviation from the expected temperature dependence of the hyperfine field. The origin of this stronger hybridization is ascribed to the relatively small magnetic anisotropy observed in $GdRh_2Si_2$ when compared with the other compounds of the series, as shown by resistance measurements.

(Some figures may appear in colour only in the online journal)

1. Introduction

The behaviour of magnetic moments at dilute magnetic atoms in metallic hosts is an interesting topic which is related to fundamental properties in condensed matter physics such as the Kondo effect. This effect, which is a striking phenomenon of the increase in the resistivity of the host metal when the temperature is lowered to nearly zero, was theoretically explained by Kondo [1] as being from the scattering of conduction electrons by the magnetic impurities.

A localized magnetic moment in metals was first observed in the early 1960s from susceptibility measurements of iron atoms diluted in 4d metals [2, 3], and then theoretically described by Anderson [4], who emphasized the nature of these moments by considering a localized resonance at the impurity.

The measurement of the magnetic hyperfine field (mhf) at the impurity soon proved to be an important tool to study localized magnetic moments at very dilute impurities in metals [5] by providing the magnitude of the moment [6]. Many experiments to measure the mhf at impurities in

magnetic hosts of metallic elements were then carried out using different hyperfine techniques, such as Mössbauer, nuclear magnetic resonance (NMR) and perturbed angular correlation (PAC) spectroscopies. The results are compiled in tables [7]. The temperature dependence of mhf at these impurities was also measured and almost all the results showed that the fields follow the temperature dependence of the host magnetization represented by a Brillouin-like curve. However, in some cases results showed strong deviations from the Brillouin curve, the first of which was observed by NMR measurements of Mn in Fe host [8]. The experimental data and its interpretation constituted the first example of a localized magnetic moment in a ferromagnetic host. Jaccarino *et al* [9] provided an explanation for the temperature dependence of the observed magnetic field at Mn impurities in terms of a molecular-field model involving a localized magnetic moment at the Mn ions which is oriented by the exchange field of Fe host. This exchange field is scaled to the reduced magnetization of the Fe host by a parameter which assumes that the intensity of the host–impurity exchange interaction is different from that of the host–host interaction. Since then similar behaviour has been observed in the magnetic hyperfine field at the nuclei of magnetic impurities in ferromagnetic elements [10–13] and in magnetic compounds [14–16]. Some slight modifications to the model proposed by Jaccarino have been added to take into account the contribution to mhf of the conduction electrons [17, 10], in order to use this model with rare-earth impurities [12] and hosts [18, 19]. Another model was proposed by Campbell [20] to explain the anomalous behaviour of mhf at d-element impurities in ferromagnetic d-element hosts. The model is based on the scattering of conduction electrons at the impurity sites, which are represented by a narrow localized d resonance situated at or near the Fermi level, and therefore can be expected to have a magnetic moment. This localized resonance is particularly sensitive to the exact electronic structure of the host, and can therefore change sharply with variation of temperature. However, no physical description of the origin of the anomalous behaviour of the mhf when the temperature varies has been given so far, which makes this an open issue yet to be resolved.

In order to fully describe the phenomenon of anomalous temperature dependence of mhf, some questions must be answered, such as: why does the same impurity in different hosts show different behaviour? Which parameters, such as distance between magnetic ion of the host and impurity, number of conduction electrons or crystal structure are important in inducing this phenomenon? It is clear that a systematic investigation is needed to answer these questions, and the best way to successfully achieve a good physical explanation of this phenomenon is to study a family of compounds. The investigation of this phenomenon in magnetic compounds of the same family has clear advantages because it is possible to separately study the influence of one specific parameter by varying the composition of the compound by changing the constituent elements within the same crystalline structure. In this way it is possible to vary the magnetic ion of the host, the distance between the magnetic ion and the impurity, the number of conduction electrons, and the position of the localized impurity band relative to the Fermi level.

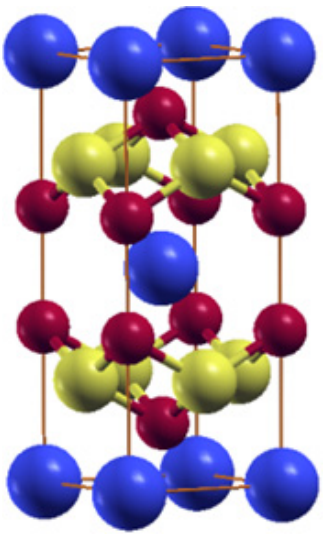

Figure 1. Crystal structure of $RERh_2Si_2$ compounds, where the blue spheres represent RE atoms, the red spheres represent Si atoms and the yellow spheres represent Rh atoms.

We thus decided to investigate, in this work, the anomalous behaviour of mhf at ^{140}Ce impurities substituting RE sites in the family of magnetic compounds $RERh_2Si_2$, where RE is Ce, Pr, Nd, Gd, Tb, Dy. The results of $CeRh_2Si_2$ and $GdRh_2Si_2$ have been reported earlier [19, 21]. The reasons for the choice of this particular impurity and this family of compounds was, first, the Ce^{3+} ion possesses only one 4f electron, which is nearer to the Fermi level than 4f electrons of the rest of the lanthanides. Such a condition makes a Ce ion quite sensitive to the chemical environment around it, and as a consequence, also sensitive to the strong interactions present around the Fermi level. Second, the family of antiferromagnetic compounds $RERh_2Si_2$, where RE is a rare-earth element, show high antiferromagnetic transition temperatures and their magnetic moments are localized solely at rare-earth ions [22]. Moreover, all these ternary rhodium-based rare-earth silicides crystallize in the well known body centred tetragonal $ThCr_2Si_2$-type structure, which belongs to the $I4/mmm$ spatial group. In this structure, RE atoms occupy $2a$ $(0, 0, 0)$ positions, the Rh atoms occupy 4d $(0, 1/2, 1/4)$ positions, forming a simple tetragonal sublattice, and the Si atoms occupy 4e $(0, 0, z)$ and $(0, 0, \bar{z})$ positions, producing, as a consequence, a compact structure formed by stacked atomic layers along the c axis with the Rh–Si–RE–Si–Rh sequence of atomic planes as shown in figure 1. This structure thus makes the interatomic distances very sensitive to changes in the constituent elements of the compounds.

All compounds investigated in this work order antiferromagnetically at unusually high Néel temperatures, which vary from the lowest 35 K for $CeRh_2Si_2$ to the highest 106 K for $GdRh_2Si_2$. Whereas the measured Néel temperatures for $GdRh_2Si_2$, $TbRh_2Si_2$ and $DyRh_2Si_2$ are

in reasonable agreement with those calculated by using the Ruderman–Kittel–Kasuya–Yosida (RKKY) theory, which predicts that the magnetic ordering temperature is proportional to the de Gennes factor $J_{sf}^2(g-1)^2J(J+1)$, some of them, such as $CeRh_2Si_2$, $PrRh_2Si_2$ and $NdRh_2Si_2$ [23], have much higher transition temperatures than the predicted values. For instance, the Néel temperature of $CeRh_2Si_2$ was measured as $T_N = 35$ K [24] and predicted to be $T_N \sim 1.5$ K. The large difference in this case has been ascribed to a mixing of itinerant and local characters of the 4f electron of Ce ions. $CeRh_2Si_2$ is indeed found to be different from the rest of the family, since it shows a superconductor behaviour at low temperatures when submitted to a pressure of 0.9 GPa [24, 25]. Despite these observations, the fact that $CeRh_2Si_2$, $PrRh_2Si_2$ and $NdRh_2Si_2$ exhibit much higher transition temperatures than predicted by RKKY theory remains largely without explanation. The magnetic properties of $PrRh_2Si_2$ was studied by several different techniques [26, 23, 27, 28] and the results show that this compound orders antiferromagnetically below ∼69 K with a magnetic moment localized at Pr, oriented parallel to the *c*-axis in a configuration which is ferromagnetic in the *a*–*b* plane and antiferromagnetic along the *c*-axis following an alternating sequence of opposite directions at the atomic positions (0, 0, 0) and (1/2, 1/2, 1/2) of Pr atoms. This behaviour seems to be widespread in the $RERh_2Si_2$ family, inasmuch as it has been also observed in $CeRh_2Si_2$ [29], $NdRh_2Si_2$ [30], $TbRh_2Si_2$ [29], and $DyRh_2Si_2$ [31, 32]. $GdRh_2Si_2$, on the other hand, was reported to order antiferromagnetically at the highest Néel temperature in the family, with magnetic moments localized at Gd atoms oriented parallel to the *a*–*b* plane, exhibiting a different behaviour when compared to the other compounds of the $RERh_2Si_2$ family.

In the present work we have investigated how the contribution from 4f electrons of Ce impurities to the mhf at ^{140}Ce can be affected by the unit cell volume of $RERh_2Si_2$ (RE = Ce, Pr, Nd, Gd, Tb, Dy) compounds and show that the volume directly influences the hybridization of d-host and f-impurity bands. We show that for $GdRh_2Si_2$ this influence strongly affects the temperature dependence of the mhf. In order to carry out this investigation, we have first characterized the samples studied in this work by x-ray diffraction (XRD), to obtain lattice parameters and the unit cell volume, and by magnetization and resistance measurements, to characterize the transport and magnetic properties. The temperature dependence of mhf at the nucleus of Ce impurities in each compound was measured by perturbed angular correlation (PAC) spectroscopy using ^{140}Ce as probe nuclei. As the structure of the $RERh_2Si_2$ family of compounds is formed by layers of the constituent atoms, the interatomic distances and the unit cell volume are quite sensitive to changes in the chemical composition. We have therefore investigated the behaviour of the measured magnetic hyperfine field at ^{140}Ce on RE sites in $RERh_2Si_2$ compounds as a function of the unit cell volume when RE elements are changed. In order to confirm the anomalous behaviour observed for $GdRh_2Si_2$, we have also carried out PAC measurements for $GdRh_2Ge_2$ for comparison.

2. Experimental procedure

The samples of $RERh_2Si_2$ (RE = Pr, Nd, Gd, Tb) were prepared from highly pure metals (99.9%) purchased from Alpha-Aesar and Si (99.9999%), by repeatedly melting the constituent elements in stoichiometric proportion in an arc furnace under argon atmosphere purified with a hot titanium getter. The samples were submitted to thermal treatment at 900 °C for a period of approximately 96 h. The radioactive ^{140}La–^{140}Ce probe was introduced in the sample by adding a small quantity of lanthanum metal (<0.1%), which had been previously irradiated with neutrons in the IEA-R1 research reactor at a neutron flux of 3×10^{13} n cm^{-2} s^{-1} for 12 h to produce ^{140}La, and the remelting the alloy in the arc furnace. The samples were once again submitted to thermal treatment at 950 °C for 72 h. The PAC measurements were carried out with a four BaF_2 detector spectrometer equipped with a slow–fast electronic set-up for measuring the delayed gamma–gamma coincidences. The gamma cascade of 328–486 keV in ^{140}Ce populated from the β^- decay of ^{140}La with an intermediate level at 2083 keV ($I^\pi = 4^+$, $T_{1/2} = 3.5$ ns) was utilized for the measurement. Since the quadrupole moment of 2083 keV state is known to be very small, one measures only the magnetic interaction with the ^{140}La–^{140}Ce probe [33]. Details of the PAC technique and experimental procedure can be found elsewhere [34]. PAC measurements were carried out in the temperature range 10–120 K.

All the samples were analysed by x-ray diffraction measurements to determine their crystal structure and lattice parameters after the radioactivity decayed almost to the background level. The zero-field resistance measurements were carried out as a function of temperature in the range 4–300 K using a four-point probe. The magnetic susceptibility was measured with externally applied magnetic field of 5 kG in the temperature range 4–300 K for the $NdRh_2Si_2$ alloys using VSM.

3. Experimental results

Spectra resulting from x-ray diffraction measurements for samples of some of the studied compounds are displayed in figure 2(a), which, within the resolution of the XRD equipment, indicate the formation of a single phase with tetragonal crystalline structure of $ThCr_2Si_2$-type belonging to the $I4/mmm$ space group. Results for lattice parameters *a* and *c* as well as for the unit cell volume (V_c) as a function of the rare-earth ions involved in this study are shown in figure 2(b). The results agree fairly well with data found in the literature [35] and show a linear decrease of the cell parameters as the rare-earth atomic number increase. This is consistent with the expected effect of lanthanide contraction.

Results of DC magnetic susceptibility measurements as a function of temperature for $NdRh_2Si_2$ are shown in figure 3, along with previously reported results for $GdRh_2Si_2$ [19], which is included in this figure for comparison. Both compounds order antiferromagnetically with Néel temperatures of $T_N = 59(1)$ K and $T_N = 106(1)$ K,

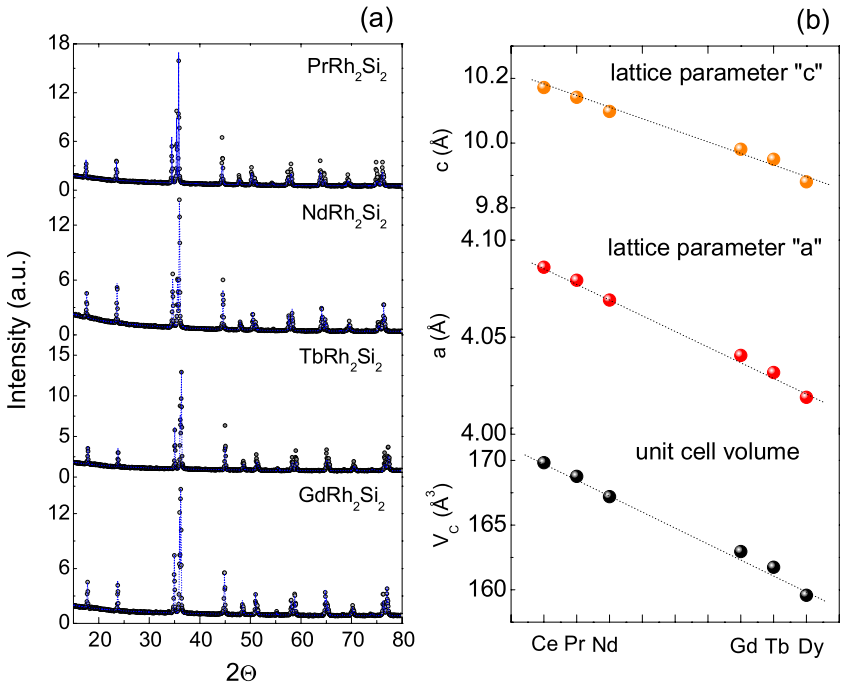

Figure 2. (a) X-ray diffraction pattern for $RERh_2Si_2$ (RE = Pr, Nd, Tb, Gd) compounds (the solid lines represent the calculated pattern with the Rietveld method), and (b) variation of lattice parameters and unit cell volume of compounds as a function of RE atoms (dashed lines are the guide to eye).

respectively, in agreement with the earlier reported values [36, 35]. Above the transition temperature, the susceptibility shows the characteristic Curie–Weiss behaviour of the paramagnetic state as the temperature is increased, described by $\chi = C/(T - \Theta_P)$. The fit of this Curie–Weiss law to the experimental data gave an effective magnetic moment $\mu_{\text{eff}} = 3.51(2)\ \mu_B$ per Nd ion for the $NdRh_2Si_2$ compound. This value is somewhat smaller than $\mu_{\text{eff}} = 3.55\ \mu_B$ for $PrRh_2Si_2$ [27]. The measured values of μ_{eff} for $TbRh_2Si_2$ and $DyRh_2Si_2$ are 8.92 μ_B [37] and 9.9 μ_B [31] respectively. In all cases the measured values are smaller than their respective calculated magnetic moment for the free 3+ rare-earth ion.

A different situation was observed for $GdRh_2Si_2$, where the measured effective magnetic moment $\mu_{\text{eff}} = 8.44(2)\ \mu_B$ per Gd ion [19] is somewhat higher than the calculated value of 7.94 μ_B. Such an increase in the magnetic moment for the $GdRh_2Si_2$ compound could be explained if a small additional magnetic moment at Rh ions is assumed. The neutron diffraction and Mössbauer spectroscopy measurements in $CeRh_2Si_2$ [38, 25], $PrRh_2Si_2$ [23, 27] and $DyRh_2Si_2$ [32] have shown, however, that there is no magnetic moment at Rh ions. It is therefore reasonable to assume that the effective magnetic moment for all the studied compounds are in fact localized only at the rare-earth ions. An alternate explanation for the higher magnetic moment at Gd ions in $GdRh_2Si_2$ was provided by Czjzek *et al* [36] as due to an additional magnetic moment induced at the 5d electrons by an 4f–5d exchange interaction which adds to the magnetic moment of the 4f electrons of Gd ions.

Some of the PAC spectra for $PrRh_2Si_2$ and $NdRh_2Si_2$, as well as for $GdRh_2Si_2$ and $TbRh_2Si_2$, measured at temperatures below T_N using ^{140}La-^{140}Ce probe nuclei are shown in figures 4 and 5, respectively. Solid curves represent the least-squares fit to the experimental data of an appropriate perturbation function for magnetic interaction defined by the

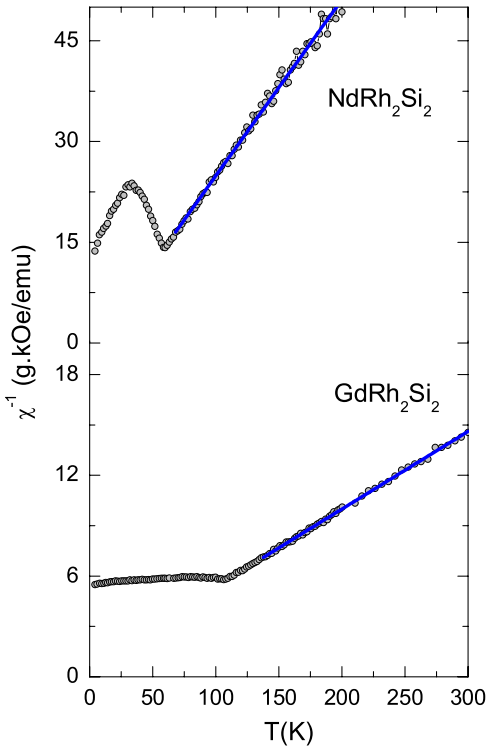

Figure 3. Reciprocal magnetic susceptibility of $NdRh_2Si_2$ (top) and $GdRh_2Si_2$ (bottom) as a function of temperature. The solid blue lines represent the data range used to fit the Curie–Weiss law to the experimental data.

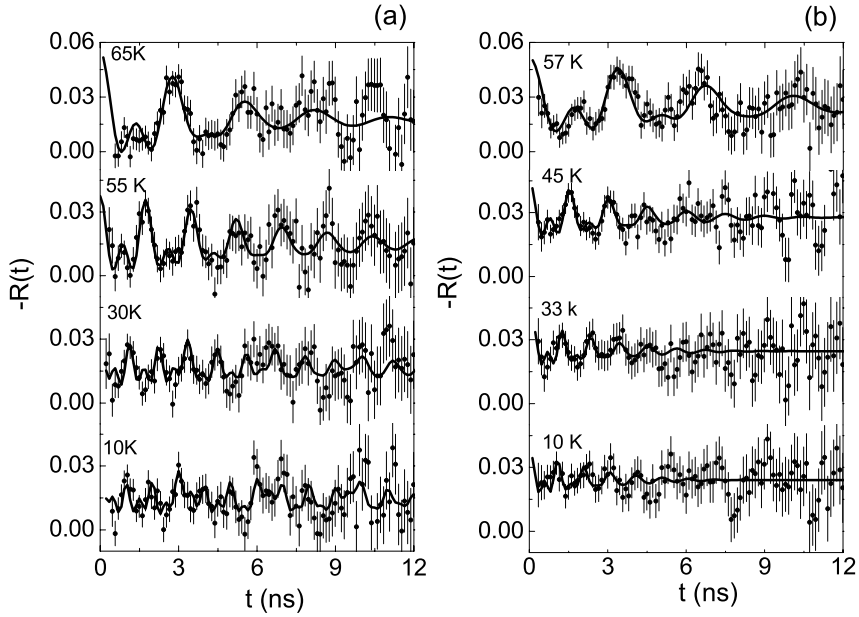

Figure 4. The PAC perturbation functions for ^{140}Ce in (a) $PrRh_2Si_2$ and (b) $NdRh_2Si_2$ compounds at indicated temperatures. The solid lines are the least-squares fits of the theoretical function to the experimental data.

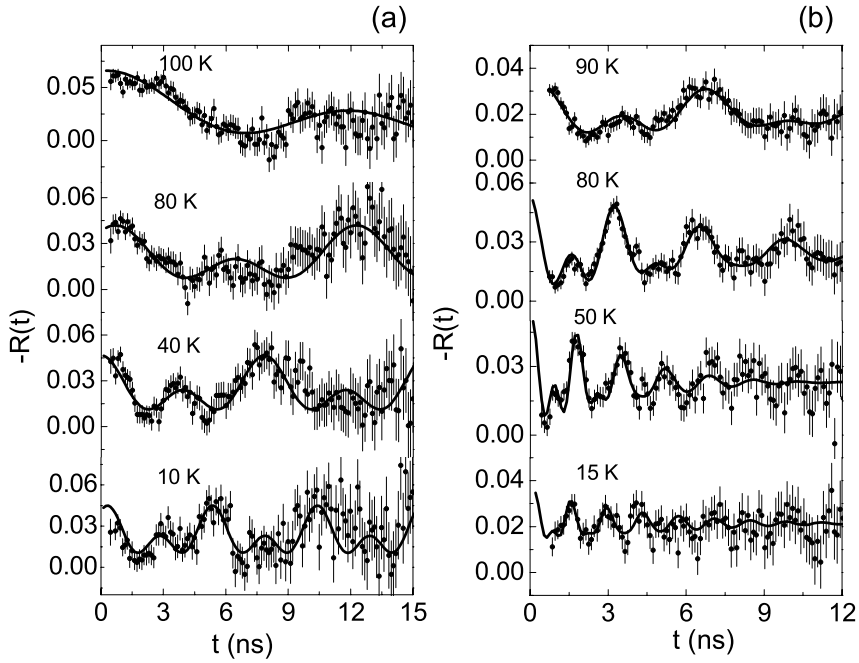

Figure 5. The PAC perturbation functions for ^{140}Ce in (a) $GdRh_2Si_2$ and (b) $TbRh_2Si_2$ compounds at indicated temperatures. The solid lines are the least-squares fits of the theoretical function to the experimental data.

following expression:

$$R(t) = A_{22}G_{22}(t) = A_{22}\sum_i f_i G^i_{22}(t), \qquad (1)$$

where A_{22} is the unperturbed angular correlation coefficient, f_i are the fractional site populations and $G^i_{22}(t)$ are the corresponding perturbation factors given by

$$G_{22}(t) = [0.2 + 0.4\cos(\omega_L t) + 0.4\cos(2\omega_L t)] \times \exp(-\omega_L^2\tau_R^2/2)\exp(-\omega_L^2\delta^2 t^2/2), \qquad (2)$$

in which the effect of finite time resolution τ_R of detectors and the distribution of mhf with a relative width δ are properly taken into account. PAC spectra were fitted with two fractions of site populations for the probe nuclei. The major fraction was assigned to probe nuclei substituting rare-earth sites in the compounds. The minor fraction, which was temperature invariant, was calculated to be 5% for $TbRh_2Si_2$ and 20% for $PrRh_2Si_2$ and $NdRh_2Si_2$, observed only at low temperatures, and 10% for $DyRh_2Si_2$, observed in all measured temperatures. We do not yet know the origin of this fraction.

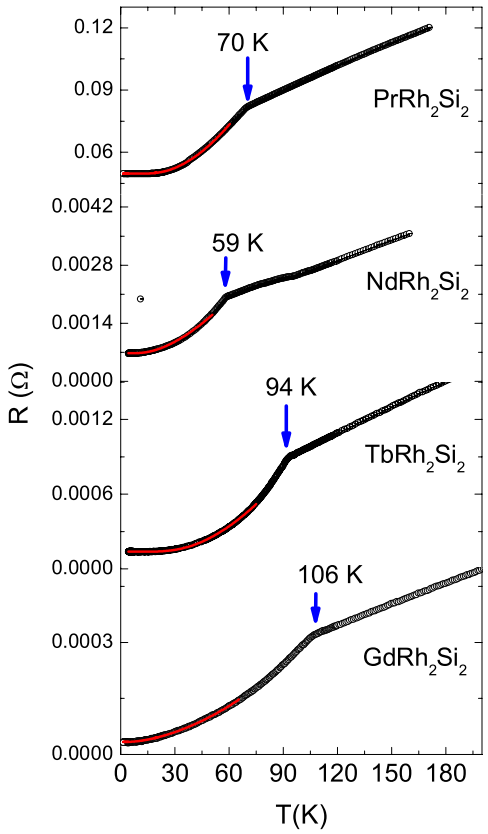

Figure 6. Resistance curves as a function of temperature for $PrRh_2Si_2$, $NdRh_2Si_2$, $TbRh_2Si_2$, and $GdRh_2Si_2$ (respectively, from top to bottom). The solid red lines represent fits using the expression given in the text to data below $T = 0.65T_N$.

Results of zero-field resistance measurements for some of the compounds are shown in figure 6 for a broad range of temperature. From these results the magnetic transition temperature (T_N) was calculated to be $T_N = 69.5$ K for $PrRh_2Si_2$, $T_N = 58.4$ K for $NdRh_2Si_2$, $T_N = 106$ K for $GdRh_2Si_2$, and $T_N = 94$ K for $TbRh_2Si_2$, as can be clearly observed in each graph. It can also be seen from the figure that above the Néel temperature for each compound, the resistance varies linearly with temperature, as expected for metallic systems, due to electron–phonon scattering.

4. Discussion

Scattering of conduction electrons by spin waves (magnon excitations) in the long-range ordered systems gives rise to an important contribution to the resistance of magnetic materials below their magnetic ordering temperatures. Since at low temperatures the resistance due to the scattering of electrons by phonons can be neglected, the spin wave contribution ($R_{SW}(T)$) is predominant and of the same order of magnitude as the total resistance ($R(T)$). Therefore, at low temperatures the total resistance of the magnetic material can be written as

$$R(T) = R_0 + R_{SW}, \tag{3}$$

where R_0 is the residual resistance at $T = 0$. The spin wave resistance can be modelled by the following equation

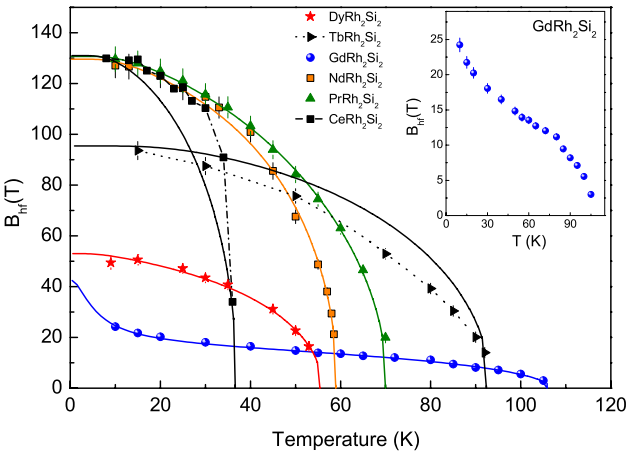

Figure 7. Temperature dependence of B_{hf} for the studied compounds. The solid lines represent the Brillouin curve for the total angular momentum J of the respective rare-earth ion in each compound, except for $GdRh_2Si_2$, for which the solid line is the fit of the model described in the text. Dotted lines are only to guide the eyes.

based on the scattering of the conduction electrons on antiferromagnetic spin waves [39]:

$$R_{SW}(T) = A\Delta^{3/2}T^{1/2}e^{-\Delta/T} \times \left[1 + \left(\frac{2}{3}\right)\left(\frac{T}{\Delta}\right) + \left(\frac{2}{15}\right)\left(\frac{T}{\Delta}\right)^2\right], \tag{4}$$

where the coefficient A is related to the spin wave velocity D ($A \propto D^{1/3}$) or to an effective magnetic coupling factor Γ between rare-earth ions in a tetragonal system ($A \propto 1/\Gamma^3$). Δ is the spin wave energy gap, which is the minimum energy required to excite spin waves from the magnetic anisotropy of the material.

The model described by (3) and (4) was fitted to experimental data for temperatures below $\sim 0.65T_N$, as shown in figure 6 by solid red lines. Results from this fitting yield a spin wave gap $\Delta = 89.5(4)$ K for $PrRh_2Si_2$, which is quite close to the value of $\Delta = 91.1(4)$ K reported in the literature for this compound [23]. The corresponding values for $NdRh_2Si_2$ and $TbRh_2Si_2$ are respectively 50.1 (5) K and 121.3 (8) K. The large spin wave gap means a strong magnetic anisotropy, which implies that the rare-earth magnetic moments in these compounds are oriented parallel to the c-axis [23]. The behaviour of resistance below T_N for $GdRh_2Si_2$ is somewhat different, as can be seen in figure 6, showing a much less pronounced curvature, almost tending to be linear. The fitted value in this case is $\Delta = 17.6(6)$ K. A linear behaviour ($\Delta \sim 0$) for the resistance has been interpreted as due to the S state of Gd ions [40]. Although the Δ value for $GdRh_2Si_2$ is much smaller than those for the other compounds, it is still large enough and indicates that there also exists an anisotropy in this system, most likely due to the strong ferromagnetic interaction between the Gd ions in the a–b plane [36].

The temperature dependence of the magnetic hyperfine field B_{hf} for the major fractions in each compound determined from PAC measurements are displayed in figure 7, along

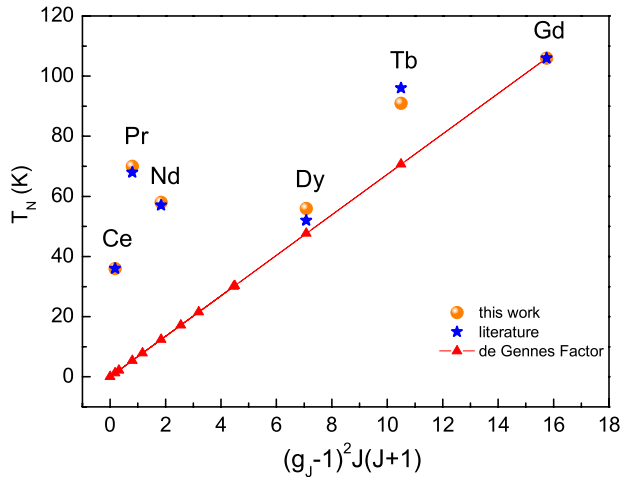

Figure 8. Néel temperature as a function of the de Gennes factor. The triangles connected by the straight solid line represent the RKKY prediction, circles are values measured in this work, and stars are data from the literature.

with previously reported data for $CeRh_2Si_2$ [21] and $GdRh_2Si_2$ [19]. One can observe from the figure that B_{hf} for every compound, except $GdRh_2Si_2$, follows a second-order Brillouin-type transition with the magnetic moments localized at rare-earth sites of the host. This behaviour indicates that the magnetic moment localized at the Ce impurity is polarized by the molecular field of the host. The behaviour of the temperature dependence of B_{hf} for $GdRh_2Si_2$ is anomalous, with a sharp deviation from the Brillouin curve, as shown in the inset of figure 7.

The extrapolation of B_{hf} versus T data to $B_{hf} = 0$ gives an estimate of T_N for each compound. The results, within the experimental uncertainties, agree with those obtained by magnetization and resistivity measurements and are quite close to the values reported in the literature, as can be seen in figure 8. These results clearly inspire confidence that the use of ^{140}La–^{140}Ce probe nuclei for measuring the hyperfine field and its temperature dependence in this series of compounds is quite adequate. In figure 8, the Néel temperature is also compared with the de Gennes factor for each compound. As reported earlier [23–26] it may be observed that T_N follows almost a linear dependence with the de Gennes factor for compounds with heavier lanthanides (Gd, Tb, and Dy), but not those with lighter lanthanides (Ce, Pr, Nd), where the experimental T_N values are considerably higher than those predicted by the de Gennes function.

The ^{140}Ce hyperfine fields measured at the lowest temperature are $B_{hf} = 129(4)$ T and $B_{hf} = 127(4)$ T for $PrRh_2Si_2$ and $NdRh_2Si_2$ respectively, both at 10 K. These values are very close to each other and also to $B_{hf} = 130(4)$ T, previously measured [21] for $CeRh_2Si_2$. The corresponding results for $TbRh_2Si_2$ and $DyRh_2Si_2$, both measured at 12 K, are $B_{hf} = 94(4)$ T and $B_{hf} = 50(4)$ T respectively. The result for $GdRh_2Si_2$ once again shows quite an anomalous behaviour, in which the measured hyperfine field at 10 K is the lowest: $B_{hf} = 24(2)$ T [19], despite the fact that this compound has the highest magnetic moment localized at rare-earth ion

Table 1. Néel temperature, effective localized magnetic moment, magnetic hyperfine field at $T = 0$ K, and spin wave energy gap values for the studied compounds.

Compound	T_N (K)	μ_{eff} (μ_B)	$B^h_{hf}(0)$ (T)	Δ (K)
$CeRh_2Si_2$	36[a] [21]	1.86 [25]	131(3)	—
$PrRh_2Si_2$	70[a], 69.5[b]	3.55 [27]	130(3)	89.5(4)
$NdRh_2Si_2$	58.8[a], 59(1)[c] 58.4[b]	3.51(2)	129(2)	50.1(5)
$GdRh_2Si_2$	106.5[a] [19], 106(1)[c] 106[b]	8.44(2) [19]	42(2)	17.6(6)
$TbRh_2Si_2$	94[a,c]	8.92 [37]	96(3)	121.3(8)
$DyRh_2Si_2$	55[a]	9.9 [31]	53(3)	—

[a] PAC.
[b] Resistance measurements.
[c] Susceptibility.

in the entire series of the studied compounds. Extrapolated values of B_{hf} to $T = 0$ K and other magnetic parameters for the studied compounds are shown in table 1.

From the results of B_{hf} measured at ^{140}Ce as a dilute impurity it is possible first to infer, from the fact that B_{hf} values for $PrRh_2Si_2$ and $NdRh_2Si_2$ are practically of the same order of magnitude as that for $CeRh_2Si_2$, where ^{140}Ce is not an impurity, that Ce impurities replace the rare-earth ions in every compound and occupy substitutional sites in the crystalline structure. Second, because the observed B_{hf} values are relatively high it is reasonable to conclude that the main contribution to the observed magnetic hyperfine field comes from the orbital magnetic moments of 4f electrons of Ce impurities. Finally, the measured B_{hf} are smaller than the magnetic hyperfine field measured for the Ce^{3+} free ion ($B_{hf} \sim 195$ T [41]).

The variation of B_{hf} as a function of rare-earth element, measured with ^{140}Ce for these compounds at the lowest temperature is quite different from that of B_{hf} measured with ^{111}Cd in rare-earth metals [42, 43] and in rare-earth based binary intermetallic compounds [44, 45]. It is also different from that measured with ^{140}Ce in rare-earth based binary [46] and ternary [47] intermetallic compounds. In all these cases the B_{hf} values increase somewhat steeply in the first half of the lanthanide series (from Ce to Eu) and then decrease slowly in the second half of the series (from Gd to Yb). From the current investigation we find the B_{hf} in $RERh_2Si_2$ are invariant in the first half of the lanthanide series (Ce, Pr, Nd) and rapidly decrease in the second half of the series (Tb, Dy). The case of Gd is anomalous and $GdRh_2Si_2$ shows the lowest B_{hf} value.

The high values of B_{hf} at ^{140}Ce probe nuclei in $PrRh_2Si_2$ and $NdRh_2Si_2$ suggest that the 4f electron at Ce probe atoms is localized, as was also shown by first-principles calculations in $CeRh_2Si_2$ [48], where it was estimated that the 4f band would be localized at 1.6 eV below the Fermi level and with a slight degree of hybridization with the 4d band. It was also reported that 4f-conduction electron hybridization is the mechanism responsible for magnetic instabilities of local magnetic moments of diluted Ce in metals [49, 50]. Hence, as Ce is a diluted impurity in the studied compounds, we believe that a similar behaviour for the Ce 4f band, which is localized

near the Fermi level and hybridized with the host d band, occurs in these compounds.

In the single impurity Anderson Model [4] the 4f band of the impurity is described as localized close to the Fermi level and hybridized with the conduction electron bands. The broadening of the f-level is given by [51]

$$\Gamma = \pi \langle |V_{\mathrm{kf}}|^2 \rangle N(\varepsilon_{\mathrm{F}}), \tag{5}$$

where V_{kf} is the average of the matrix element of the impurity potential between the 4f orbital and the conduction electron k orbitals, and $N(\varepsilon_{\mathrm{F}})$ is the conduction electron density of states at the Fermi level. The f and k conduction electron states are therefore mixed by V_{kf}, which accounts for the hybridization between these states and it is inversely proportional to the unit cell volume of the compound [4].

The influence of hybridization on the magnetic hyperfine field can be investigated by considering that the effective hyperfine field (B_{hf}) measured at ^{140}Ce probes can basically be considered as a sum of the 4f-impurity field ($B_{4\mathrm{f}}$) and the host contribution (B_{host}), and can be written as [52]

$$B_{\mathrm{hf}} = B_{4\mathrm{f}} + B_{\mathrm{host}}. \tag{6}$$

The host contribution comes from the neighbouring magnetic ions, which is proportional to the effective magnetic moment (μ_{eff}) at the magnetic ions [53, 34]. As the contribution to B_{hf} from the host via conduction electron polarization depends mainly on the number of conduction electrons [34], which is practically the same for all $RERh_2Si_2$ compounds, the reduced magnetic hyperfine field ($B_{\mathrm{hf}}/\mu_{\mathrm{eff}}$) can, therefore, be used as a parameter to investigate the behaviour of $B_{4\mathrm{f}}$ through the series of $RERh_2Si_2$ compounds. In figure 9 the reduced magnetic hyperfine field ($B(0)_{\mathrm{hf}}/\mu_{\mathrm{eff}}$), where $B(0)_{\mathrm{hf}}$ is the extrapolated value of B_{hf} to $T = 0$ K, is plotted as a function of the unit cell volume for the $RERh_2Si_2$ compounds. The experimental data, excluding that of $GdRh_2Si_2$, were fitted to a second-order polynomial function shown as a solid red line in the figure. In the same figure, the effective localized moment (μ_{eff}) at the rare-earth ion for each compound is also plotted as a function of the unit cell volume. It can be seen that μ_{eff} decreases linearly with the unit cell volume of $RERh_2Si_2$ compounds in going from Dy to Ce (blue dashed straight line in the figure). Since μ_{eff} shows a linear dependence with the volume, it is therefore clear that, with the exception of $GdRh_2Si_2$, $B(0)_{\mathrm{hf}}/\mu_{\mathrm{eff}}$ follows a systematic behaviour as a function of volume. As $B(0)_{\mathrm{hf}}/\mu_{\mathrm{eff}}$ monotonically decreases as the unit cell volume of the compound decreases from $CeRh_2Si_2$ to $DyRh_2Si_2$, we suggest that the $B_{4\mathrm{f}}$ decreases as a consequence of hybridization of the 4f state of the Ce impurity, which is located closer to the Fermi level than the 4f state of the rare-earth ions of the host, with the s and d bands of the host. This hybridization results in a widening of the 4f band of the Ce impurity, as predicted by the Anderson model. When the volume decreases, from $CeRh_2Si_2$ to $DyRh_2Si_2$, the 4f band broadens and, consequently, part of it becomes delocalized reducing the contribution of the orbital magnetic field of the impurity to B_{hf}.

An important result is that the value of $B(0)_{\mathrm{hf}}/\mu_{\mathrm{eff}}$ for $GdRh_2Si_2$ is well below that expected from the curve

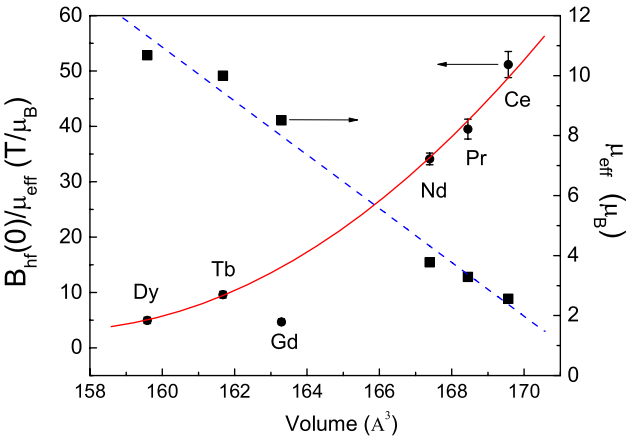

Figure 9. The reduced magnetic hyperfine field as a function of the unit cell volume of the studied compounds. The solid line is the fit of a second-order polynomial function to the data. The magnetic moment localized at the rare-earth sites in the compounds is also plotted as squares. The dashed line is a linear fit to the magnetic moment data.

shown in figure 9, which indicates that the hybridization of the 4f state of the Ce impurity is much stronger than that for the other compounds. As a consequence of this strong hybridization, the Ce-impurity 4f band, according to (6), is thus quite wide, and therefore the delocalization of this band is more intensified than that observed in the other compounds. We suggest that the reason for such behaviour is due to the position of the hybridized d bands of Gd and Rh of the host relative to the Fermi energy. First-principles calculations suggest that a substantial part of the 5d band of Gd is located above the Fermi level, and the 4d band of Rh is situated below the Fermi level [54, 55]. In particular, the hybridization for $5d_{xy}$ and $5d_{yz}$ orbitals is larger than for the other 5d orbitals because they are directed towards the position of Rh in the crystalline structure. Thus the hybridized 5d–4d band extends through the Fermi level. The 4f band of the Ce impurity is also located in the same region of the d bands of the host, and the strong hybridization with such bands make it broad, resulting in a delocalization of part of the 4f band, with a consequent decrease in the $B_{4\mathrm{f}}$.

First-principles calculations also show that the behaviour of d bands of Gd and Rh are quite similar in $GdRh_2Si_2$ and $GdRh_2Ge_2$ [55]. Therefore, if there is a difference in the volume of these compounds, according to Anderson's prediction, the hybridization will be different, and, consequently, the $B_{4\mathrm{f}}$ measured with ^{140}Ce probes should also be different, as we suggested above. In order to check this point, we prepared a sample of $GdRh_2Ge_2$ doped with neutron irradiated La metal, following the same procedure used to prepare $GdRh_2Si_2$ described earlier. The crystal structure of the sample was investigated by x-ray diffractometry and the result, shown in figure 10, yields values of $a = 4.108(1)$ Å, $c = 10.307(1)$ Å, and a volume of 174 Å^3. This value for the volume agrees quite well with the value of 176 Å^3 reported in the literature [56], and is ∼6.6% larger than that for $GdRh_2Si_2$.

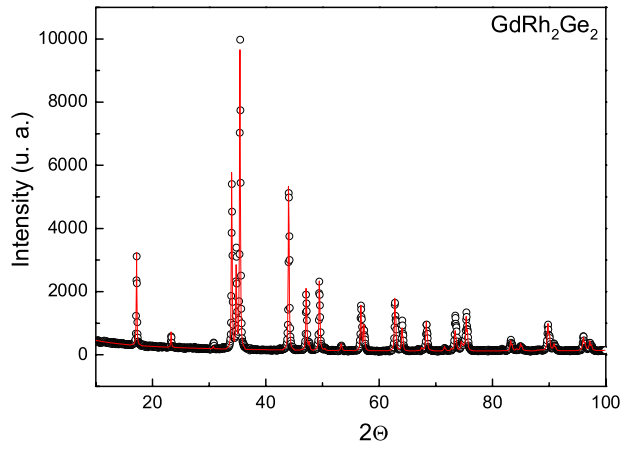

Figure 10. X-ray diffraction pattern for $GdRh_2Ge_2$. The solid line represent the calculated pattern with the Rietveld method.

The magnetic hyperfine field at ^{140}Ce in $GdRh_2Ge_2$ was measured as a function of temperature, and the results are shown in figure 11. In the plot of the temperature dependence of B_{hf}, data for $GdRh_2Si_2$ are also shown for comparison (see figure 11(b)).

The temperature dependence of B_{hf} for $GdRh_2Ge_2$ and $GdRh_2Si_2$ are quite similar, as can be seen in figure 11. Both compounds display the same anomalous behaviour. This behaviour is a consequence of the strong interaction between the magnetic ions of the host and the 4f electron of the Ce impurity [19], which is polarized by the exchange field of the host [15]. A simple model based on the molecular-field theory, first proposed by Jaccarino *et al* [9] and modified to apply to the case of Ce impurities in rare-earth based magnetic compounds [57, 19], can be used to quantitatively describe the behaviour of the temperature dependence of B_{hf}. In this model the hyperfine field at the probe site is given by $B_{hf} = B_i + B_h$, where B_i is the contribution from the impurity ion, which is the ^{140}Ce probe in the present case, and B_h is the contribution from the magnetic field of rare-earth ions of the host, which scales with the host reduced magnetization $\sigma(T)$. B_i is proportional to the thermal average of the impurity magnetic moment J_i, which is localized. The magnetic hyperfine field at the impurity site is thus written as

$$B_{hf}(T) = B_i(0) \times B_{J_i}(y) + B_h(0)\sigma(T), \tag{7}$$

where $B_{Ji}(y)$ is the Brillouin function and y is its argument given by

$$y = \frac{\mu_B(g_{J_i} - 1)\vec{J}_i \cdot \vec{B}_{exc}(T)}{kT}. \tag{8}$$

In this expression, $B_{exc}(T)$ is the exchange field, which also scales with $\sigma(T)$, and is given by

$$B_{exc}(T) = \frac{3kT_0\xi}{(g_{J_h} - 1)(J_h + 1)\mu_B} \times \sigma(T), \tag{9}$$

where T_0 is the magnetic transition temperature, μ_B is the Bohr magneton, and k is the Boltzmann constant. The parameters $g_{J_h} = 2$ and $J_h = 7/2$ are, respectively, the Landè factor and total angular momentum of the Gd ion. Lastly, the parameter ξ takes into account the fact that the host–impurity exchange interaction strength may be different from that of the host–host exchange.

The parameters produced by the fit of this model to the experimental data of $B_{hf}(T)$ measured with ^{140}Ce in $GdRh_2Ge_2$ are $B_i(0) = -31$ T, $B_h(0) = 14$ T, $T_0 = 91$ K, and

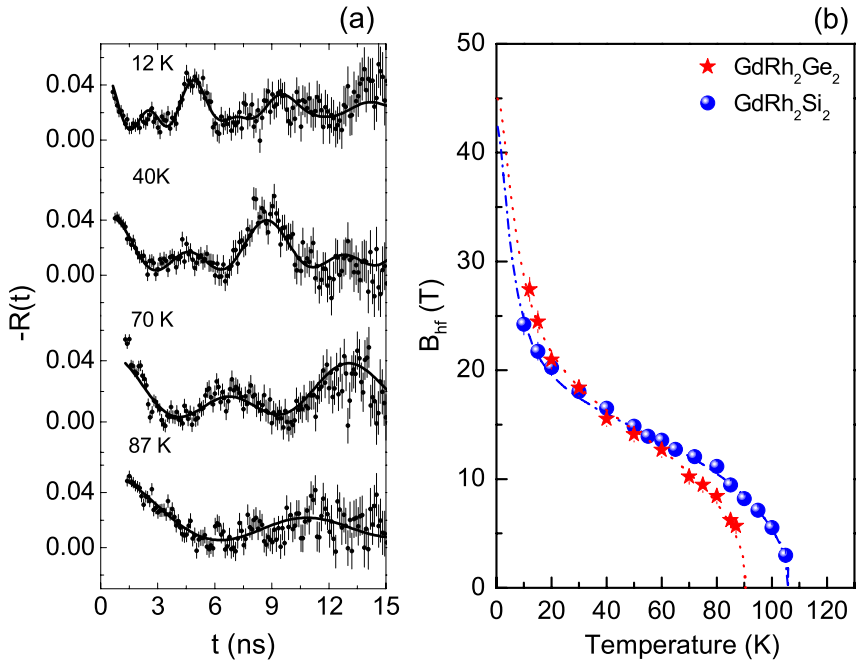

Figure 11. (a) The PAC perturbation functions for ^{140}Ce in $GdRh_2Ge_2$ at indicated temperatures. (b) Temperature dependence of B_{hf} for $GdRh_2Ge_2$. Similar results for $GdRh_2Si_2$ are also shown for comparison.

$\xi = 0.091$. The parameters obtained previously for $GdRh_2Si_2$ are $B_i(0) = -28$ T, $B_h(0) = 12.4$ T, $T_0 = 107$ K, and $\xi = 0.056$ [19]. It can be noticed that the transition temperatures T_0, which in both compounds represents the Néel temperature, agrees quite well with the values found in the literature [36, 56]. Moreover, the values of $B_i(0)$ represent the contribution of the 4f electron to B_{hf}, i.e. the B_{4f} contribution. The absolute value of this contribution to the B_{hf} in $GdRh_2Ge_2$ is 7.1% larger than that of B_{hf} in $GdRh_2Si_2$, which is very close to the value of 6.6% found for the volume ratio of $GdRh_2Ge_2$ to $GdRh_2Si_2$. This result completely follows the Anderson's prediction: the larger is the volume, the weaker is the hybridization, and, consequently the larger is the B_{4f} contribution. Therefore, B_{4f} is directly proportional to the volume of the unit cell of the compound. A very good agreement between the variation of $B_i(0)$ for $GdRh_2Ge_2$ and $GdRh_2Si_2$ with the variation of the respective unit cell volume of the compounds, which according to (5) is proportional to the width of 4f band with a consequent effect on B_{4f}, therefore shows that the model described by (7) is capable of correctly estimating the impurity contribution to B_{hf}.

The anomalous behaviour of the temperature dependence of B_{hf} measured at probe nuclei of magnetic elements as diluted impurities in magnetic hosts is an old issue but not well settled yet. This anomaly has been observed in several experiments of hyperfine interaction measurements since Koi *et al* first reported experimental data of the temperature dependence of NMR frequencies of ^{55}Mn impurities in an iron host [8]. Similar behaviour of the temperature dependence of magnetic hyperfine field was observed in transition-metal impurities in transition-metal hosts, such as ^{99}Ru in Ni [10], s–p impurities in transition-metal hosts, for instance ^{119}Sn in Co [11], rare-earth impurities in transition-metal hosts, such as ^{169}Tm in Fe [12] and ^{140}Ce in Co [58], and rare-earth impurities in rare-earth hosts, for instance ^{140}Ce in Gd [13]. More recently, this phenomenon was also observed at rare-earth impurities in rare-earth magnetic compounds: ^{169}Tm in $TmFe_2$ [59], ^{140}Ce in RAg [16, 60, 57] and ^{140}Ce in $CeMn_2Ge_2$ [15]. The investigation of this phenomenon in magnetic compounds has advantages because it is possible to separately study the influence of one specific parameter by varying the composition of the compound within the same crystalline structure. In the present work, it was possible to find an important clue to explain the origin of the observed anomaly in the temperature dependence of B_{hf}. We suggest that the hybridization of the 4f band of the Ce impurity with d bands of the host, which are polarized by the magnetic Gd ions, is responsible for the exchange interaction between the spins of the magnetic ions of the host and the Ce impurities. The exchange interaction between the 4f electrons of Gd and Ce is mediated by the wide d band, which extends beyond the Fermi level. As a result, at higher temperatures more and more of d electrons are promoted to the conduction band, which weakens this exchange interaction, and as a consequence decreases the B_{4f} contribution, which is dominant in the total B_{hf}. This mechanism, therefore, results in a strong deviation of the temperature dependence of the magnetic hyperfine field from the standard Brillouin-like curve at higher temperatures.

5. Conclusions

New results of the temperature dependence of hyperfine fields measured with PAC spectroscopy, using a ^{140}Ce probe, for the intermetallic compounds $PrRh_2Si_2$, $NdRh_2Si_2$, $TbRh_2Si_2$ and $DyRh_2Si_2$ are reported. These results along with the previous data on $CeRh_2Si_2$ and $GdRh_2Si_2$ compounds are discussed together to understand the anomalous behaviour of the temperature dependence of hyperfine field at ^{140}Ce highly diluted in $GdRh_2Si_2$ and $GdRh_2Ge_2$. This anomalous behaviour has been observed in several other magnetic systems in which the magnetic hyperfine field is measured at diluted magnetic probe atoms, but so far the origin of this phenomenon has not been well understood. Additional measurements of zero-field resistance and magnetic susceptibility were also carried out in these compounds, which together with the PAC results confirmed magnetic transition temperatures in good agreement with the literature values.

We have addressed the question whether the contribution from 4f electrons of Ce impurities to the mhf at ^{140}Ce could be influenced by the unit cell volume of the $RERh_2Si_2$ compounds when the rare-earth atom changes, showing that the unit cell volume directly influences the hybridization of d-host and f-impurity bands. For $GdRh_2Si_2$, this influence strongly affects the temperature dependence of the mhf. It is further shown that the hybridization of the 4f band of the Ce impurity with the d bands of the host, which are polarized by the magnetic ions, is responsible for the exchange interaction between the spins of the magnetic ions of the host and the Ce impurities. The hybridization is stronger in $GdRh_2Si_2$ in comparison with other compounds and is responsible for the observed anomalous behaviour of the temperature dependence of the hyperfine field in this compound. The origin of the strong hybridization is most likely due to the relatively small magnetic anisotropy observed in $GdRh_2Si_2$ compared with other compounds, as shown by the resistance measurement data.

Acknowledgments

Partial support for this research was provided by the Fundação de Amparo à Pesquisa do Estado de São Paulo (FAPESP). AWC, BBS, JMF and RNS gratefully acknowledge the support provided by CNPq in the form of research fellowships. The authors thank E. M. Baggio-Saitovitch of Centro Brasileiro de Pesquisas Físicas (CBPF) for help with the resistance measurements and J.A.H. Coaquira of University of Brasília, Instituto de Física, Núcleo de Física Aplicada for magnetic susceptibility measurements.

References

[1] Kondo J 1964 *Prog. Theor. Phys.* **32** 37–49
[2] Matthias B T, Peter M, Williams H J, Clogston A M, Corenzwit E and Sherwood R C 1960 *Phys. Rev. Lett.* **5** 542
[3] Clogston A M, Matthias B T, Peter M, Williams H J, Corenzwit E and Sherwood R C 1962 *Phys. Rev.* **125** 541
[4] Anderson P W 1961 *Phys. Rev.* **124** 41

[5] Craig P P, Nagle D E, Steyert W A and Taylor R D 1962 *Phys. Rev. Lett.* **9** 12
[6] Freeman A J 1963 *Phys. Rev.* **130** 888
[7] Rao G N 1985 *Hyperfine Interact.* **24–26** 1119
[8] Koi Y, Tsujimura A and Hihara T 1964 *J. Phys. Soc. Japan* **19** 1493
[9] Jaccarino V, Walker L R and Wertheim G K 1964 *Phys. Rev. Lett.* **13** 752
[10] Shirley D A, Rosenblum S S and Matthias E 1968 *Phys. Rev.* **170** 363
[11] Huffman G P and Dunmyre G R 1970 *J. Appl. Phys.* **41** 1323
[12] Bernas H and Gabriel H 1973 *Phys. Rev.* B **7** 468
[13] Thiel T A, Gerdau E, Böttcher M and Netz G 1981 *Hyperfine Interact.* **9** 459
[14] Bleaney B, Bowden G J, Cadogan J M, Day R K and Dunlop J B 1982 *J. Phys. F: Met. Phys.* **12** 79
[15] Carbonari A W, Mestnik-Filho J, Saxena R N and Lalic M V 2004 *Phys. Rev.* B **69** 144425
[16] Cavalcante F H M, Carbonari A W, Saxena R N and Mestnik-Filho J 2005 *Hyperfine Interact.* **158** 125
[17] Low G G 1966 *Phys. Lett.* **21** 497
[18] Wäckelgard E, Karlsson E, Lindgren B, Mayer A and Hrynkiewicz Z 1989 *Hyperfine Interact.* **51** 853
[19] Cabrera-Pasca G A, Carbonari A W, Saxena R N, Bosch-Santos B, Coaquira J A H and Filho J A 2012 *J. Alloys Compounds* **515** 44
[20] Campbell I A 1970 *J. Phys. C: Solid State Phys.* **3** 2151
[21] Cabrera-Pasca G A, Carbonari A W, Saxena R N and Bosch-Santos B 2010 *J. Appl. Phys.* **107** 09E141
[22] Szytula A and Leciejewicz J 1989 *Handbook on the Physics and Chemistry of Rare Earths* vol 12, ed K A Gschneidner Jr and L Eyring (Amsterdam: Elsevier) p 133
[23] Szytula A, Kaczorowski D, Gondek L, Arulraj A, Baran S and Penc B 2008 *Solid State Commun.* **146** 61
[24] Graf T, Hundley M F, Modler R, Movshovich R, Thompson J D, Mandrus D, Fisher R A and Phillips N E 1998 *Phys. Rev.* B **57** 7442
[25] Kawarazaki S, Sato M, Miyako Y, Chigusa N, Watanabe K, Metoki N, Koike Y and Nishi M 2000 *Phys. Rev.* B **61** 4167
[26] Anand V K, Hossain Z, Behr G, Chen C and Geibel C 2007 *J. Phys.: Condens. Matter* **19** 506205
[27] Hossain Z, Rajarajan A K, Anand V K, Geibel C and Yusuf S M 2009 *J. Magn. Magn. Mater.* **321** 213
[28] Shigeoka T, Fujiwara T, Koyama K, Watanabe K and Uwatoko Y 2010 *J. Low Temp. Phys.* **159** 42
[29] Quezel S, Rossat-Mignod J, Chevalier B, Lejay P and Etourneau J 1984 *Solid State Commun.* **49** 685
[30] Szytula A, Slaski M, Ptasiewicz-Bak H, Leciejewicz J and Zygmunt A 1984 *Solid State Commun.* **52** 395
[31] Melamud M, Pinto H, Felner I and Shaked H 1984 *J. Appl. Phys.* **55** 2034
[32] Tomala K, Sanchez J P and Kmiec R 1989 *J. Phys.: Condens. Matter* **1** 9231
[33] Bosch-Santos B, Cabrera-Pasca G A and Carbonari A W 2010 *Hyperfine Interact.* **197** 105
[34] Carbonari A W, Saxena R N, Pendl W Jr, Mestnik-Filho J, Atilli R N, Olzon-Dionysio M and de Souza S D 1996 *J. Magn. Magn. Mater.* **163** 313
[35] Felner I and Nowik I 1983 *Solid State Commun.* **47** 831
[36] Czjzek G, Oestreich V, Schmidt H, Latka K and Tomala K 1989 *J. Magn. Magn. Mater.* **79** 42
[37] Slaski M, Leciejewicz J and Szytula A 1983 *J. Magn. Magn. Mater.* **39** 268
[38] Grier B H, Lawrence J M, Murgai V and Parks R D 1984 *Phys. Rev.* B **29** 2664
[39] Continentino M A, de Medeiros S N, Orlando M T D, Fontes M B and Baggio-Saitovitch E M 2001 *Phys. Rev.* B **64** 012404
[40] Fontes M B, Trochez J C, Giordanengo B, Budko S L, Sanchez D R, Baggio-Saitovitch E M and Continentino M A 1999 *Phys. Rev.* B **60** 6781
[41] Barth H J, Netz G, Nishiyama K and Riegel D 1980 *Phys. Rev. Lett.* **45** 1015
[42] Forker M and Hammesfahr A 1973 *Z. Phys.* **263** 33
[43] Forker M 1985 *Hyperfine Interact.* **24** 907
[44] de la Presa P, Müller S, Pasquevich A F and Forker M 2000 *J. Phys.: Condens. Matter* **12** 3423
[45] Müller S, de la Presa P and Forker M 2004 *Hyperfine Interact.* **158** 163
[46] Saitovitch H, Silva P R J, Carbonari A W, Mestnik-Filho J and Lalic M V 2004 *J. Magn. Magn. Mater.* **272** 631
[47] Lapolli A L, Saxena R N, Mestnik-Filho J, Leite D M T and Carbonari A W 2007 *J. Appl. Phys.* **101** 09D510
[48] Vildosola V, Llois A M and Alouani M 2005 *Phys. Rev.* B **71** 184420
[49] Barth H J, Luszik-Bhadra M and Riegel D 1983 *Phys. Rev. Lett.* **50** 608
[50] Büermann L, Barth H J, Biedermann K H, Luszik-Bhadra M and Riegel D 1986 *Phys. Rev. Lett.* **56** 492
[51] Schrieffer J R and Wolff P A 1966 *Phys. Rev.* **149** 491
[52] Netz G 1986 *Z. Phys.* B **63** 343
[53] Campbell I A 1969 *J. Phys. C: Solid State Phys.* **2** 1338
[54] Coehoorn R, Buschow K H J, Dirken M W and Thiel R C 1990 *Phys. Rev.* B **42** 4645
[55] Mulder F M, Thiel R C and Buschow K H J 1993 *J. Alloys Compounds* **202** 169
[56] Felner I and Nowik I 1985 *J. Phys. Chem. Solids* **46** 681
[57] Cavalcante F H M, Pereira L F D, Carbonari A W, Mestnik-Filho J and Saxena R N 2010 *J. Magn. Magn. Mater.* **322** 1130
[58] Carbonari A W, Cabrera-Pasca G A, Saxena R N and Mestnik-Filho J 2007 *Hyperfine Interact.* **176** 69
[59] Bleaney B, Bowden G J, Cadogan J M, Day R K and Dunlop J B 1982 *J. Phys. F: Met. Phys.* **12** 79
[60] Carbonari A W, Cavalcante F H M, Pereira L F D, Cabrera-Pasca G A, Mestnik-Filho J and Saxena R N 2008 *J. Magn. Magn. Mater.* **320** e478